

Loading of g-C₃N₄ on Core-Shell Magnetic Mesoporous Silica Nanospheres as a Solid Base Catalyst for the Green Synthesis of some Chromene Derivatives under Different Conditions

Shekofeh Neamani and Leila Moradi*^[a]

Using heterogeneous basic catalysts has a great importance in chemical reactions because of their advantages (such as easy separation and thermal stability at harsh conditions) over homogeneous catalysts. In this study, magnetic mesoporous silica nanoparticles (mSiO₂) containing graphitic carbon nitride layers (mSiO₂/g-C₃N₄(x)) were fabricated through a facile process (x signifies the amount of melamine applied during synthesis). Graphitic carbon nitride layers were decorated on mSiO₂ by calcination of immobilized melamine (as graphitic carbon

nitride precursor) on mSiO₂ in the last step of catalyst synthesis. The structure of the prepared catalysts was confirmed using XRD, BET, FESEM, EDX, elemental mapping and TEM methods. The catalytic efficiency of the so-obtained solid base composite was investigated for the synthesis of some dihydropyranochromenes and spiro-dihydropyranochromenes under thermal and microwave conditions. Using mSiO₂/g-C₃N₄(x) led to high yields under green conditions and in short reaction times and without a decrease in catalytic activity after four consecutive cycles.

Introduction

Nowadays, improving the utilization of catalysts in the synthesis of organic compounds has become an important topic. Chemical reactions developed by the base catalysis are great processes for many of fine chemical productions. In this respect, aldol and Knoevenagel condensations are of the most important carbon-carbon bond establishment reactions.^[1,2] Basic catalysts comprise both homogeneous and heterogeneous base catalysts. Heterogeneous catalysts were applied to defeat the problems affected by homogeneous ones. The possibility of reusing these catalysts over and over again makes them suitable in chemical reactions. Also, using such catalysts makes the corresponding reactions more environmentally friendly.^[3-8] The activity of base catalysts depends on their number of basic sites.^[9] Basic sites at the catalyst surfaces can include functional groups anchored to their surface, edges and also structural defects. Recently, it has been demonstrated that structural defects in heterogeneous catalysts play a considerable role in their catalytic properties.^[10,11] Defects, for catalysts, means deviations of the real crystal structure relative to the ideal

lattice structure. The study of defects in catalyst supports activity became a significant topic in the catalyst field. Defects in heterogeneous catalysts have diverse types owing to the different crystalline structures of catalysts. For instance, several defect sorts which include edges, vacancies, and pentagon defects can exist in carbon-based catalysts, influencing catalytic activity.^[10-13]

Carbon nitrides are a group of polymeric materials that mainly contain carbon and nitrogen atoms. Carbon nitride layers, due to having attractive surface features and active basic sites, have been found excellent candidates for use in various catalysis fields.^[14-17]

Generally, graphitic carbon nitrides (g-C₃N₄) are obtained from the thermal polymerization of nitrogen-containing precursors at high temperatures. Studies have shown that incomplete polymerization during the formation of g-C₃N₄ layers leads to structural defects in the overall g-C₃N₄ structures, which result in increasing the number of edges and defects in the final g-C₃N₄ structure. Increasing the g-C₃N₄ structural defects can then bring about improved basic properties and activity of the final structure of g-C₃N₄ layers.^[18,19]

Heating is one of the main methods developed by scientists to destroy the regular structure of g-C₃N₄. Indeed, at high temperatures, the strong covalent bonds between carbon and nitrogen in tri-s-triazine units do not change, but hydrogen bonds between graphite carbon nitride plates are gradually weakened, which leads to a change in angle and the rotation of the corresponding plates. In consequence, irregular short units with basic features forms are obtained.^[15,18,20] It is necessary to mention that applying of g-C₃N₄ as a catalyst in catalytic process has some restrictions and problems. One of them is the low specific surface area of g-C₃N₄ which is due to its high agglomeration property. In fact, once the layers of g-C₃N₄ form, they assemble on top of each other and aggregations occur

[a] Dr. S. Neamani, Dr. L. Moradi
Department of Organic Chemistry
Faculty of Chemistry
University of Kashan
P.O. Box 8731753153
Kashan, I. R. (Iran)
E-mail: l_moradi@kashanu.ac.ir

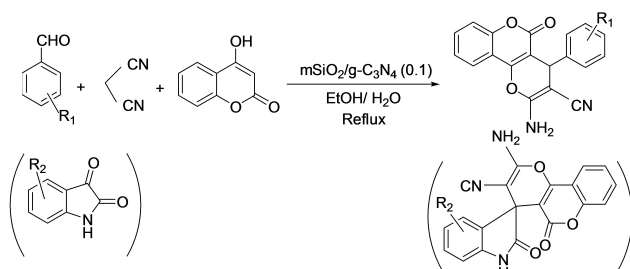
Supporting information for this article is available on the WWW under <https://doi.org/10.1002/open.202200041>

© 2022 The Authors. Published by Wiley-VCH GmbH. This is an open access article under the terms of the Creative Commons Attribution Non-Commercial NoDerivs License, which permits use and distribution in any medium, provided the original work is properly cited, the use is non-commercial and no modifications or adaptations are made.

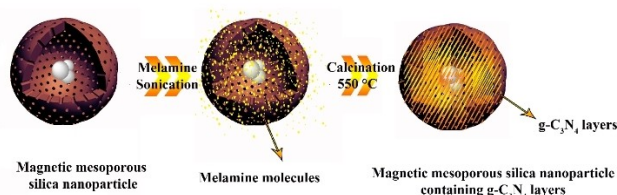
that result in poor catalytic activity.^[15,21] Thus, restricting the formation of long layers of g-C₃N₄ can cause to break them to the short chains which cater numerous structural defects and high specific surface area on its layers.^[21,22] In this regard, mesoporous silica nanoparticles (NPs), due to their properties such as high surface areas (more than 700 m²g⁻¹), high chemical and thermal stability, appropriate particle size (2 to 10 nm), specific morphology and controllable porosity, are a useful option for catalyst support.^[23–25] By using mesoporous silica as a support for the formation of g-C₃N₄ layers in their pores, incomplete polymerization occurs, causing an increase in the number of structural defects, edges and basic features. Furthermore, loading of g-C₃N₄ in the pores of magnetic mesoporous silica NPs can make them easy to separate from the reaction medium.

In this contribution, this method was thus successfully used to prepare an efficient basic heterogeneous catalyst. The obtained catalyst was employed in the preparation of some dihydropyranochromene and spiro-dihydropyranochromene derivatives through the environmentally friendly method in green solvents (Scheme 1) which are desirable from the point of green chemistry.^[26]

Due to special properties of chromene derivatives such as anti-HIV, anti-tuberculosis, antioxidants anti-cancer, antiseptic and anti-inflammatory (in the field of medicinal chemistry), they have attracted much attention in recent years.^[27–35] Furthermore, the interest in chromenes bearing an additional nitrile functionality arises from their potential application in the treatment of human inflammatory TNF α -mediated diseases, such as rheumatoid and psoriatic arthritis, and in cancer therapy.^[36–39] Thus, new methods for the preparation of these compounds are of interest in organic and pharmaceutical syntheses.



Scheme 1. Synthesis of pyrano[2,3-c]chromene and spiro-pyrano[2,3-c]chromene derivatives in the presence of mSiO₂/g-C₃N₄(0.1).



Scheme 2. Synthesis of mSiO₂/g-C₃N₄ composite.

Results and Discussion

Catalyst Characterization

The procedure applied for the synthesis of mSiO₂/g-C₃N₄ composite is presented in Scheme 2. After preparation of magnetic mesoporous silica nanoparticles (mSiO₂) (according to our previous work^[23]), acidic solution of melamine as a precursor of g-C₃N₄ was added to the synthesized mSiO₂ NPs. Therefore, most of the melamine molecules stuck into the channel pores and on the surfaces of mSiO₂ NPs. Then, calcination of the obtained solids at 550 °C caused incomplete structure formation of the g-C₃N₄ layers inside the channel pores and on the surface of the mSiO₂ NPs.

Different amounts of melamine, namely 0.05, 0.1 and 0.15 g, were used to prepare the mSiO₂/g-C₃N₄(0.05), mSiO₂/g-C₃N₄(0.1) and mSiO₂/g-C₃N₄(0.15) composites, respectively. In the following, the structure of mSiO₂/g-C₃N₄(0.1) as the high performance catalyst was studied. Figure 1 shows FESEM images of mSiO₂ and of the mSiO₂/g-C₃N₄(0.1) composite. As can be seen in Figure 1 (a, b), mSiO₂ NPs have spherical morphology. Against, in the synthesized catalysts (Figure 1(c, d)), due to formation of graphitic carbon nitride layers in channels as well as on the surfaces of mSiO₂ NPs, more cumulative structures are observed.

The elemental mapping analysis of mSiO₂/g-C₃N₄(0.1) is shown in Figure 2. As can be seen, next to the presence of Si, O, and Fe from mSiO₂, the presence of nitrogen and carbon atoms (from g-C₃N₄) with good dispersion on the mSiO₂ surfaces was well proved.

To study the phase and crystalline structure of the mSiO₂/g-C₃N₄(0.1), powder X-ray diffraction (XRD) patterns of mSiO₂ and mSiO₂/g-C₃N₄(0.1) were compared (Figure 3).

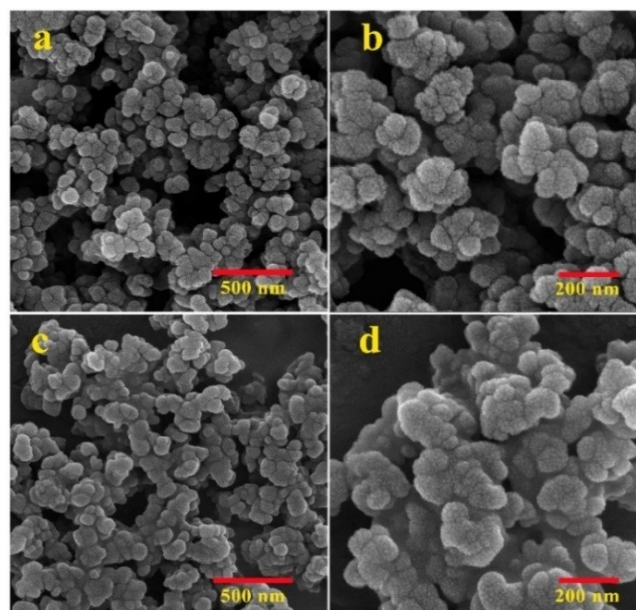


Figure 1. FESEM images of (a, b) mSiO₂ NPs and (c, d) mSiO₂/g-C₃N₄(0.1).

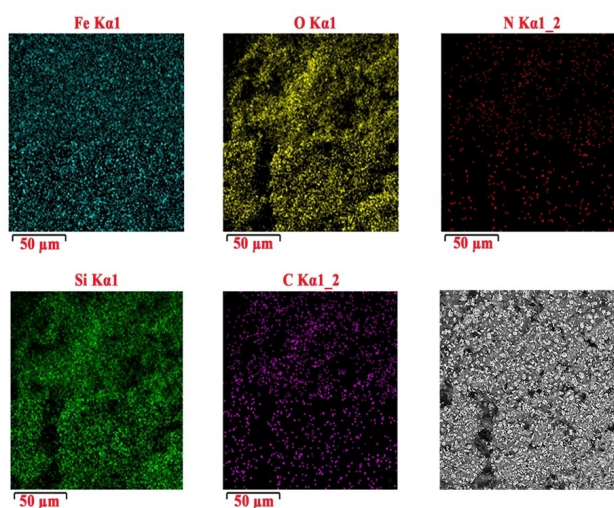


Figure 2. Elemental mapping of $m\text{SiO}_2/\text{g-C}_3\text{N}_4(0.1)$.

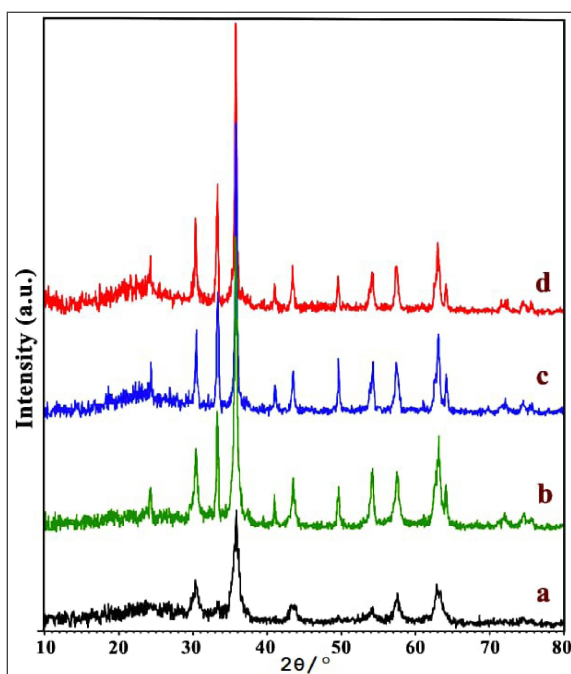


Figure 3. X-ray diffraction patterns of (a) $m\text{SiO}_2$ NPs, (b) $m\text{SiO}_2/\text{g-C}_3\text{N}_4(0.05)$, (c) $m\text{SiO}_2/\text{g-C}_3\text{N}_4(0.1)$ and (d) $m\text{SiO}_2/\text{g-C}_3\text{N}_4(0.15)$.

In the diffractogram of $m\text{SiO}_2$ (Figure 3a), a broad peak in the region of $2\theta \approx 21\text{--}28^\circ$ indicates the amorphous structure of silica. In the diffractogram of $m\text{SiO}_2/\text{g-C}_3\text{N}_4(0.1)$, graphitic carbon nitride has two clear peaks at 13.1 and 27.4° which are related to the (100) and (002) planes of the carbon nitride structure, respectively.^[14,15] These peaks show repetitive tri-s-triazine structures and accumulations of aromatic carbon plates in the graphitic carbon nitride. According to the literature,^[14] these peaks, in the absence of long carbon chains of graphitic carbon nitride, begin to weaken and widen, which in fact indicates the amorphous structure for graphite carbon nitride. The presence of a peak at around 27.4° for all of three

synthesized catalysts confirms the formation of carbon nitride plates in amorphous forms. Other peaks in the X-ray diffraction spectrum in all samples are associated to the presence of Fe_3O_4 NPs as well as to Fe_2O_3 NPs which are formed by surface oxidation of Fe_3O_4 NPs in the furnace.^[40]

Nitrogen gas adsorption and desorption isotherms as well as BJH-plots for $m\text{SiO}_2$ and $m\text{SiO}_2/\text{g-C}_3\text{N}_4(0.1)$ are shown in Figure 4. Obtained information from BET analysis of these samples is presented in Table 1. The obtained data show that $m\text{SiO}_2$ and $m\text{SiO}_2/\text{g-C}_3\text{N}_4(0.1)$ have a specific surface area of 361 and $168 \text{ m}^2\text{g}^{-1}$, respectively. The decrease in surface area of the prepared catalyst compared to $m\text{SiO}_2$ is due to the filling of pores and also due to covering of the silica NP surface by the $\text{g-C}_3\text{N}_4$ layers. The increase of average pore diameter is due to the porous structure of $\text{g-C}_3\text{N}_4$ attached to the $m\text{SiO}_2$ NPs.

Figure 5 shows the TEM images of $m\text{SiO}_2/\text{g-C}_3\text{N}_4(0.1)$. As can be seen, silica NPs containing Fe_3O_4 NPs have been successfully formed. Also, layers of $\text{g-C}_3\text{N}_4$ on the surface and into the channel pores of $m\text{SiO}_2$ were well dispersed.

Catalytic Performance for the Synthesis of Chromene Derivatives

In order to optimize the reaction conditions in the presence of the catalyst, the reaction of 4-hydroxycoumarin, 4-nitrobenzaldehyde and malononitrile was selected as the model reaction. Then (as shown in Table 2), the efficiency of synthesized catalysts with some homogeneous catalysts in different solvents were compared for this model reaction (Entries 1–7). The results show that, for the model reaction, $m\text{SiO}_2/\text{g-C}_3\text{N}_4(0.1)$ in 10 mL ethanol under reflux conditions had the highest efficiency (about 84%) compared to other homogeneous catalysts. In the following, the effect of water as a co-solvent for ethanol was investigated (Entries 8–11). According to the obtained results, a volume ratio of water to ethanol (3:7) showed the best performance (Entry 11). Also, increasing the temperature from 80 to 90°C has not obvious effect on the efficiency of reaction (Entries 11, 12). Finally, the basic activity of prepared catalysts containing different amounts of graphitic carbon nitride was investigated (Entries 11, 14, 15). As is clear, by increasing the amount of melamine as a precursor of $\text{g-C}_3\text{N}_4$, the catalytic activity of synthesized catalyst was increased. It is, however, assumed that the accumulation of $\text{g-C}_3\text{N}_4$ layers in $m\text{SiO}_2/\text{g-C}_3\text{N}_4(0.15)$ rather than for $m\text{SiO}_2/\text{g-C}_3\text{N}_4(0.1)$ caused a decrease in basic sites concentration and thus a decline in the catalytic activity of the catalyst. Consequently, 15 mg of catalyst ($m\text{SiO}_2/\text{g-C}_3\text{N}_4(0.1)$) in $\text{H}_2\text{O}/\text{Ethanol}$ (3:7) at 80°C was identified the optimum reaction conditions.

Table 1. Obtained results from BET analysis.

Sample	BET surface area [m^2g^{-1}]	Total pore volume [cm^3g^{-1}]	Average pore diameter [nm]
$m\text{SiO}_2$	361	0.37	4.1
$m\text{SiO}_2/\text{g-C}_3\text{N}_4(0.1)$	168	0.34	8.1

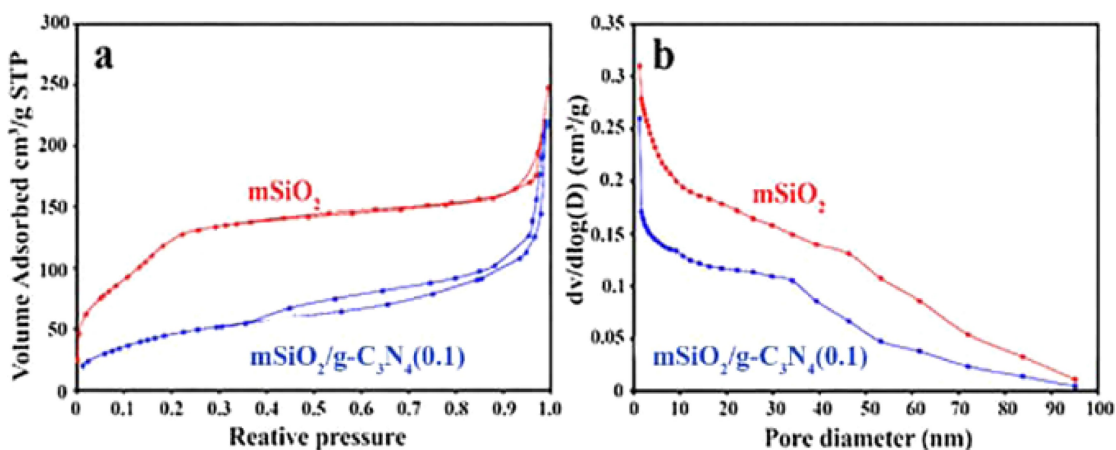


Figure 4. The N₂ adsorption-desorption isotherms of: mSiO₂ and mSiO₂/g-C₃N₄(0.1).

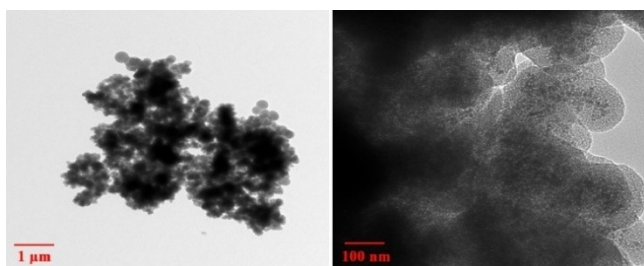


Figure 5. TEM images of mSiO₂/g-C₃N₄(0.1).

In the following, mSiO₂/g-C₃N₄(0.1) as the best catalyst was used to prepare some chromene derivatives (Table 3). In this way, some pyrano- and spiro-pyranochromenes were prepared through the multi-component reaction of 4-hydroxycoumarin,

malononitrile and benzaldehyde (isatin) in 10 mL of water and ethanol with a volume ratio of 3:7 in the presence of 15 mg mSiO₂/g-C₃N₄(0.1) as the solid base catalyst. The reaction was performed under thermal and also microwave conditions (Scheme 1). Products were obtained in high to excellent yields and their structure was investigated by FTIR spectroscopy as well as by ¹H NMR and ¹³C NMR analysis. The achieved results are presented in Table 3.

As shown in Table 3, different derivatives of benzaldehyde and isatin were used in the reaction to investigate the effect of electron-donating and -withdrawing groups on the reaction efficiency. As can be seen, the presence of electron-withdrawing groups on the phenyl ring of benzaldehyde and isatin structures increases the efficiency of reaction, and the presence of electron-donating groups on the benzaldehyde structure reduces the reaction efficiency both under thermal and micro-

Table 2. Optimization of solvent, temperature and catalyst.^[a]

Entry	Solvent	Catalyst (Loading)	Temperature	Yield [%]
1	EtOH	–	Reflux	0
2	EtOH	Et ₃ N (10 mol%)	Reflux	68
3	EtOH	L-Prolin (10 mol%)	Reflux	62
4	EtOH	(NH ₄) ₂ HPO ₄ (10 mol%)	Reflux	55
5	CHCl ₃	Et ₃ N (10 mol%)	Reflux	61
6	CH ₃ CN	Et ₃ N (10 mol%)	Reflux	65
7	EtOH	mSiO ₂ /g-C ₃ N ₄ (0.1) (15 mg)	Reflux	84
8	H ₂ O/Ethanol (9:1)	mSiO ₂ /g-C ₃ N ₄ (0.1) (15 mg)	Reflux (80 °C)	88
9	H ₂ O/Ethanol (7:3)	mSiO ₂ /g-C ₃ N ₄ (0.1) (15 mg)	Reflux (80 °C)	91
10	H ₂ O/Ethanol (5:5)	mSiO ₂ /g-C ₃ N ₄ (0.1) (15 mg)	Reflux (80 °C)	89
11	H ₂ O/Ethanol (3:7)	mSiO ₂ /g-C ₃ N ₄ (0.1) (15 mg)	Reflux (80 °C)	93
12	H ₂ O/Ethanol (3:7)	mSiO ₂ /g-C ₃ N ₄ (0.1) (15 mg)	Reflux (90 °C)	91
13	H ₂ O/Ethanol (3:7)	mSiO ₂ /g-C ₃ N ₄ (0.1) (10 mg)	Reflux (80 °C)	86
14	H ₂ O/Ethanol (3:7)	mSiO ₂ /g-C ₃ N ₄ (0.05) (15 mg)	Reflux (80 °C)	20
15	H ₂ O/Ethanol (3:7)	mSiO ₂ /g-C ₃ N ₄ (0.15) (15 mg)	Reflux (80 °C)	82

[a] Reaction conditions: carbonyl (1 mmol), malononitrile (1 mmol), 4-hydroxycoumarin (1 mmol) in 10 mL solvent at reflux for 8 h.

Table 3. Investigation of mSiO₂/g-C₃N₄(0.1) for the synthesis of pyrano and spiropyranochromenes.^[a]

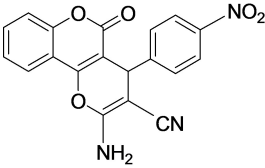
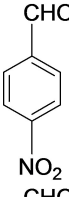
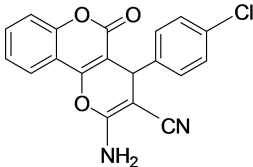
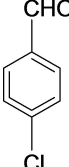
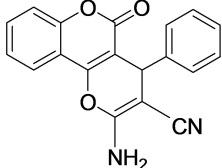
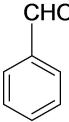
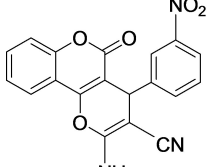
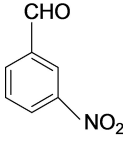
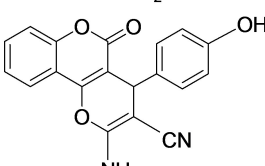
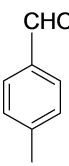
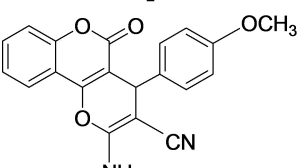
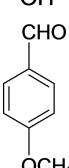
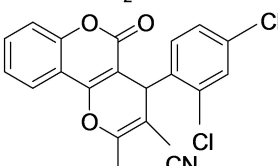
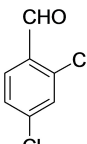
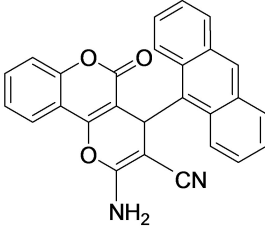
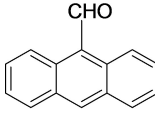
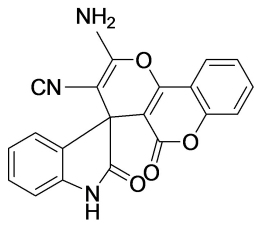
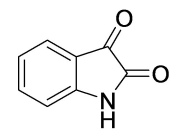
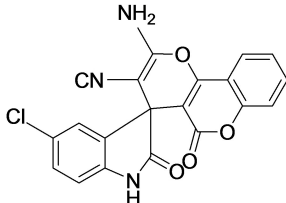
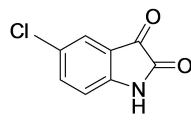
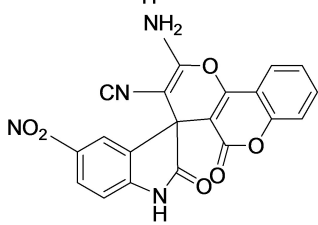
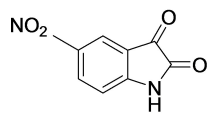
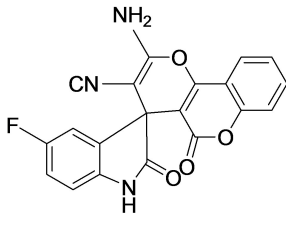
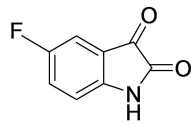
MW Time [min] / Yield [%]	Thermal Time [h] / Yield [%]	Product	Aldehyde/Isatin	Entry
10/95	4/93			1
8/88	5/87			2
12/79	6/81			3
8/94	4/92			4
15/81	7/85			5
13/80	7/80			6
10/87	7/89			7
16/84	8/86			8

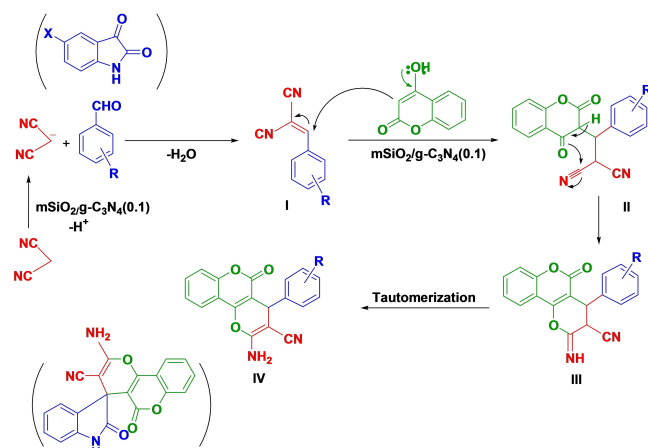
Table 3. continued				
MW Time [min] / Yield [%]	Thermal Time [h] / Yield [%]	Product	Aldehyde/Isatin	Entry
11/87	9/88			9
9/89	9/89			10
8/94	8/92			11
8/91	8/90			12

[a] Reaction conditions: benzaldehyde (isatin) (1 mmol), malononitrile (1 mmol), 4-hydroxycoumarin (1 mmol) in 10 mL EtOH/H₂O (7:3) and 15 mg mSiO₂/g-C₃N₄(0.1) at 80 °C (thermal conditions) / 600 W (microwave conditions).

wave conditions. Furthermore, using the microwave method, all of performed reactions were done in shorter times in comparison to thermal conditions.

Reaction Mechanism

For the preparation of dihydropyranochromenes derivatives, 4-hydroxycoumarin, malononitrile, benzaldehyde and for the preparation of spiro-dihydropyranochromene, 4-hydroxycoumarin, malononitrile and isatin in the presence of mSiO₂/g-C₃N₄(0.1) catalyst were reacted under both thermal and microwave conditions. Based on similar work done for the mentioned multi-component reaction, the following mechanism is presented in Scheme 3.^[27] At first, the solid base catalyst captures the proton of active methylene of malononitrile for a Knoevenagel condensation with benzaldehyde (or isatin) to form the intermediate (I). After that, a Michael addition by nucleophilic attack of 4-hydroxycoumarin to intermediate (I) produces the intermediate (II) and then an intramolecular cyclization causes the formation of intermediate (III). Finally, a tautomerization in (III) produces the desired product (IV).



Scheme 3. Proposed mechanism for the synthesis of chromenes using mSiO₂/g-C₃N₄(0.1)

Ensuring the capability of reusing heterogeneous base catalysts for repeated cycles is a significant challenge in their design and use. The ease of separation and reusing them is a very important feature. Therefore, the prepared magnetic

mSiO₂/g-C₃N₄(0.1) was separated from the reaction medium by a magnet and was washed several times with water and ethanol. Then, after drying, it was used again in the same reaction. The results showed that, after four cycles, there was no significant change in the efficiency of catalyst and the yield of product (Figure 6).

A study on the activity of prepared catalyst compare to the other reported works has been done and results were collected in Table 4. As can be seen, mSiO₂/g-C₃N₄(0.1) shows considerable efficiency both with respect to reaction time and yield of product when compare to others (Entry 6, 10).

Conclusion

In the present study, magnetic mesoporous silica NPs containing graphitic carbon nitride layers (mSiO₂/g-C₃N₄) were fabricated using different amounts of melamine (as a precursor of graphitic carbon nitride). In the prepared catalysts, amorphous structure of g-C₃N₄ trapped in the holes of mesoporous silica NPs (consisting of numerical basic sites), revealed them to be

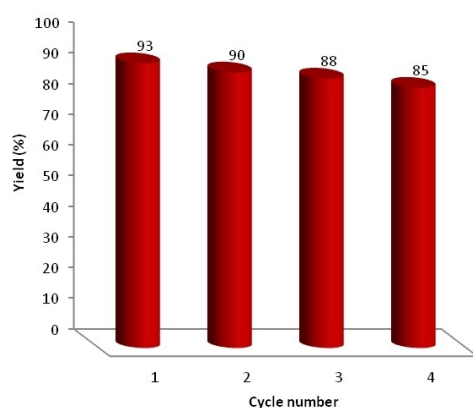


Figure 6. Reusability of mSiO₂/g-C₃N₄(0.1).

Entry	Reaction conditions	Yield (%)	Ref.
1	Sodium citrate in ethanol/water at 20 °C, 10 min	95	[41]
2	Tetrabutylammonium bromide on water at 80 °C, for 0.25 h;	85	[42]
3	Aq. buffer (pH 4.5) at 40 °C, 15 h	85	[43]
4	Acetonitrile at 50 °C, 3 h	72	[44]
5	DMAP, 150 °C, 0.33 h; microwave irradiation;	85	[45]
6	mSiO ₂ /gC ₃ N ₄ , U.S., r.t., 10 min	95	This work
7	PTSA In water for 6 h, Reflux	85	[46]
8	Carbon sheets with sulfonic acid, thanol, 80 °C, 5 h	86	[47]
9	magnetic nano-sized copper ferrite, H ₂ O/EtOH, 95 °C, 85 min.	90	[48]
10	mSiO ₂ /gC ₃ N ₄ , U.S., r.t., 8 min	94	This work

[a] Entries 1 to 6: reaction conditions for the preparation of product "a"; entries 7 to 10: reaction conditions for the synthesis of product "k".

an appropriate choice for catalytic reactions. The synthesized catalysts were used successfully to prepare some dihydropyranochromene and spiro-dihydropyranochromene derivatives. The mSiO₂/g-C₃N₄(0.1) catalyst was found to display the best efficiency for the synthesis of dihydropyranochromene and spirodihydropyranochromene under both heating and microwave conditions in the green solvents. Also, the catalyst showed proper reusability in the repeatable cycles.

Experimental Section

Materials and Apparatuses

Hydrochloric acid solution (37%), potassium permanganate (KMnO₄), tetraethyl orthosilicate (TEOS), cetrimonium bromide (CTAB), FeCl₂·4H₂O and FeCl₃·6H₂O, melamine and all solvents were purchased from Sigma-Aldrich. 4-Hydroxycoumarin, benzaldehyde derivatives, Isatin derivatives, malononitrile and ammonia solution (25%), as well as the commercial thin-layer chromatography (TLC) plates (silica gel 60 F254) were purchased from Merck. Chemicals were used directly without any further purification.

To study the crystalline structure of the obtained composites, X-ray diffraction patterns were measured using a Philips X'pert MPD diffractometer with a copper target working at the current of 100 mA and a voltage of 45 kV, with Cu-Kα radiation (λ = 0.154056 nm) on a 2θ = 10–70° scanning range at the speed of 0.05 °/min. The N₂ adsorption/desorption analysis (BET) was done to control the specific surface area of the synthesis catalyst composites by using an automated gas adsorption analyzer (Tristar 3000, Micromeritics) at –196 °C. The surface morphology of the attained catalysts was investigated by a Mira3-XMU field emission scanning electron microscope (FESEM) instrument with the scanning electron electrode at 15 kV. The morphology of synthesized catalysts was studied by TEM technique by a PhilipsCM 120, Netherlands, microscope with an accelerating voltage of 150 kV. FTIR spectra were recorded as KBr pellets in the range of 400–4000 cm⁻¹ on a Perkin-Elmer 781 spectrophotometer and on an impact 400 Nicolet FTIR. ¹H NMR and ¹³C NMR spectra were recorded in DMSO-d₆ solvent on a Bruker DRX-400 spectrometer. The chemical shifts were reported as parts per million (ppm) and tetramethylsilane (TMS) was applied as internal reference. The melting points of all derivatives were detected using an Electro-thermal Mk3 apparatus.

Synthesis of Magnetic Fe₃O₄ Nanoparticles

Conforming our prior work,^[23] 0.085 g FeCl₂·4H₂O and 0.2 g FeCl₃·6H₂O (the molar ratio of Fe³⁺/Fe²⁺ being equal to 1.75) were added into 50 mL of deionized water at 85 °C. Next, ammonia solution (0.6 mL) was added to the mixture and stirred under an inert nitrogen atmosphere at 85 °C for 30 min. Finally, the prepared magnetic NPs were separated with an external magnetic field, washed with DI water and ethanol and dried at room temperature.

Synthesis of Magnetic Mesoporous Silica Nanoparticles (mSiO₂)

The preparation of mSiO₂ nanoparticles was done according to our previous work.^[23] 0.1 g of the synthesized magnetic NPs and 0.7 g CTAB were added into 160 mL of deionized water and the mixture was sonicated for 10 min in a bath sonicator. Then, the obtained mixture was added to 220 mL of ethanol containing 1.2 mL of the

NH₃ solution (25%). Next, TEOS solution (0.4 mL TEOS in 10 mL ethanol) was added dropwise to the above mixture under stirring. The so-obtained mixture was stirred for 12 h at room temperature. The collected magnetic NPs were separated by an external magnetic field and washed several times with ethanol. Resulted solid was calcinated at 550 °C for 6 h to obtain mSiO₂.

Synthesis of Magnetic Mesoporous Silica NPs Containing Graphitic Carbon Nitride Layers (mSiO₂/g-C₃N₄)

For the synthesis of magnetic mesoporous silica nanoparticles containing graphitic carbon nitride layers, the different amounts of melamine (including 0.05, 0.1 and 0.15 g) in acidic solution (melamine dissolved in 20 mL water and 2 mL hydrochloric acid) were added to 0.1 g of the prepared mSiO₂ NPs. The resultant mixture was sonicated and then stirred at 50 °C to evaporate the solvent. In the following, the obtained solid was put in a furnace at 550 °C for 4 h at a ramp rate of 5 °C min⁻¹. Fabricated catalysts were labeled as mSiO₂/g-C₃N₄(x), with x defined as the amount of applied melamine as the precursor of graphitic carbon nitride layers. In this regard, mSiO₂/g-C₃N₄(0.05), mSiO₂/g-C₃N₄(0.1) and mSiO₂/g-C₃N₄(0.15) were prepared.

Catalyst Performance for the Synthesis of Chromene Derivatives under Thermal and Microwave Conditions

To synthesis of pyrano[2,3-c]chromene and spiroprano[2,3-c]chromene derivatives, equimolar amounts of 4-hydroxycoumarin, malononitrile and benzaldehyde or isatin (for spiro products) in the presence of 15 mg of synthesized catalyst in a mixture of DI water and ethanol (as an environmentally friendly solvent; 10 mL of 3:7 volume ratio, respectively) at 80 °C were reacted under reflux conditions. The progress of the reaction was monitored by TLC. After the end of the reaction, the catalyst was separated by an external magnetic field. The obtained solid product was filtered and washed with water and ethanol to remove unreacted substrates. The identity of the so-obtained products was completely confirmed by FTIR, ¹H NMR and ¹³C NMR spectra information consistent in comparison with authentic samples.^[27,48–51]

For the synthesis of chromene derivatives under microwave conditions, equimolar amounts of 4-hydroxycoumarin, malononitrile and benzaldehyde or isatin (for spiro products) in the presence of 15 mg of prepared catalyst in 10 mL of green solvent (3:7 volume ratio of H₂O/EtOH) was reacted under microwave irradiation with a power of 600 W for an appropriate time. The progress of reaction was monitored by TLC. The separation of reaction products was carried as previously described for the thermal condition procedure.

Acknowledgements

We are grateful to the University of Kashan for supporting this work by grant number 1073180.

Conflict of Interest

The authors declare no conflict of interest.

Data Availability Statement

The data that support the findings of this study are available in the supplementary material of this article.

Keywords: basic catalyst · dihydropyranochromenes · graphitic carbon nitride · magnetic mesoporous silica nanoparticles · spiro-dihydropyranochromenes

- [1] F. Su, M. Antonietti, X. Wang, *Catal. Sci. Technol.* **2012**, *2*, 1005–1009.
- [2] K. Ebitani, K. Motokura, K. Mori, T. Mizugaki, K. Kaneda, *J. Org. Chem.* **2006**, *71*, 5440–5447.
- [3] S. Neamani, L. Moradi, M. Sun, *Appl. Surf. Sci.* **2020**, *504*, 144466–144477.
- [4] S. Ernst, M. Hartmann, S. Sauerbeck, T. Bongers, *Appl. Catal. A* **2000**, *200*, 117–123.
- [5] S. H. Y. S. Abdullah, N. H. M. Hanapi, A. Azid, R. Umar, H. Juahir, H. Khattoon, A. Endut, *Renewable Sustainable Energy Rev.* **2017**, *70*, 1040–1051.
- [6] L. Zhu, X. Q. Liu, H. L. Jiang, L. B. Sun, *Chem. Rev.* **2017**, *117*, 8129–8176.
- [7] L. Jameie, A. Shahzeydi, M. Ghiaci, M. Sun, *J. Environ. Chem. Eng.* **2021**, *9*, 105086–105095.
- [8] L. Moradi, M. Zare, *Green Chem. Lett. Rev.* **2018**, *11*, 197–208.
- [9] H. Alshammari, M. Alhumaimess, M. H. Alotaibi, A. S. Alshammari, *J. King Saud Univ. Sci.* **2017**, *29*, 561–566.
- [10] C. Xie, D. Yan, H. Li, S. Du, W. Chen, Y. Wang, Y. Zou, R. Chen, S. Wang, *ACS Catal.* **2020**, *10*, 11082–11098.
- [11] J. Maier, *Angew. Chem. Int. Ed.* **1993**, *32*, 313–335; *Angew. Chem.* **1993**, *105*, 333–354.
- [12] J. Jia, C. Qian, Y. Dong, Y. F. Li, H. Wang, M. Ghossoub, K. T. Butler, A. Walsh, G. A. Ozin, *Chem. Soc. Rev.* **2017**, *46*, 4631–4644.
- [13] J. Zhu, Y. Huang, W. Mei, C. Zhao, C. Zhang, J. Zhang, I. S. Amiinu, S. Mu, *Angew. Chem. Int. Ed.* **2019**, *58*, 3859–3864; *Angew. Chem.* **2019**, *131*, 3899–3904.
- [14] A. Shahzeydi, M. Ghiaci, H. Farrokhpour, A. Shahvar, M. Sun, M. Saraji, *Chem. Eng. J.* **2019**, *370*, 1310–1321.
- [15] J. Zhu, P. Xiao, H. Li, S. A. C. Carabineiro, *ACS Appl. Mater. Interfaces* **2014**, *6*, 16449–16465.
- [16] Z. Huang, F. Li, B. Chen, T. Lu, Y. Yuan, G. Yuan, *Appl. Catal. B.* **2013**, *136*, 269–277.
- [17] N. S. Rizi, A. Shahzeydi, M. Ghiaci, L. Zhang, *J. Environ. Chem. Eng.* **2020**, *8*, 104219–104231.
- [18] W. J. Ong, L. L. Tan, Y. H. Ng, S. T. Yong, S. P. Chai, *Chem. Rev.* **2016**, *116*, 7159–7329.
- [19] Y. Kang, Y. Yang, L. C. Yin, X. Kang, G. Liu, H. M. Cheng, *Adv. Mater.* **2015**, *27*, 4572–4577.
- [20] A. Thomas, A. Fischer, F. Goettmann, M. Antonietti, J. O. Müller, R. Schlögl, J. M. Carlsson, *J. Mater. Chem.* **2018**, *18*, 4893–4908.
- [21] Z. Yang, Y. Zhang, Z. Schnepf, *J. Mater. Chem. A.* **2015**, *3*, 14081–14092.
- [22] T. O. Ajiboye, A. T. Kuvarega, D. C. Onwudiwe, *Nano-Struct. Nano-Objects* **2020**, *24*, 100577–100599.
- [23] S. Neamani, L. Moradi, M. Sun, *RSC Adv.* **2020**, *10*, 35397–406.
- [24] K. Sugino, N. Oya, N. Yoshie, M. Ogura, *J. Am. Chem. Soc.* **2011**, *133*, 20030–20032.
- [25] A. Shahzeydi, M. Ghiaci, L. Jameie, M. Panjepour, *Appl. Surf. Sci.* **2019**, *485*, 194–203.
- [26] S. Neamani, L. Moradi, *ChemistrySelect* **2020**, *5*, 7439–7446.
- [27] J. M. Khurana, B. Nand, P. Saluja, *Tetrahedron* **2010**, *66*, 5637–5641.
- [28] C. S. Konkoy, D. B. Fick, S. X. Cai, N. C. Lan, J. F. W. Keana, *PCT Int. Appl. WO Patent 0075123*, *Chem. Abstr.* **2001**, *134*, 29313a.
- [29] Y. K. Al-Majedy, A. A. H. Kadhum, A. A. Al-Amiery, A. B. Mohamad, *Syst. Rev. Pharm.* **2017**, *8*, 62–70.
- [30] B. C. Raju, R. N. Rao, P. Suman, P. Yogeewari, D. Sriram, T. B. Shaik, S. V. Kalivendi, *Bioorg. Med. Chem. Lett.* **2011**, *21*, 2855–2859.
- [31] P. Gebhardt, K. Dornberger, F. A. Gollmick, U. Gräfe, A. Härtl, H. Görls, B. Schlegel, C. Hertweck, *Bioorg. Med. Chem. Lett.* **2007**, *17*, 2558–2560.
- [32] N. Noroozi Pesyan, G. Rezanejade Bardajee, E. Kashani, M. Mohammadi, H. Batmani, *Res. Chem. Intermed.* **2020**, *46*, 347–367.
- [33] K. Ojaghi Aghbash, N. Noroozi Pesyan, H. Batmani, *Appl. Organomet. Chem.* **2019**, *33*, e5227.
- [34] K. Ojaghi Aghbash, N. Noroozi Pesyan, E. Şahin, *Res. Chem. Intermed.* **2019**, *45*, 2079–2094.

- [35] K. Ojaghi Aghbash, N. Noroozi Pesyan, G. Marandi, N. Dege, E. Sahin, *Res. Chem. Intermed.* **2019**, *45*, 4543–4554.
- [36] J. Skommer, D. Wlodkowic, M. Matto, M. Eray, J. Pelkonen, *Leukemia Res.* **2006**, *30*, 322–331.
- [37] W. Kemnitzer, S. Kasibhatla, S. Jiang, H. Zhang, J. Zhao, S. Jia, L. Xu, C. Crogan-Grundy, R. Denis, N. Barriault, L. Vaillancourt, S. Charron, J. Dodd, G. Attardo, D. Labrecque, S. Lamothe, H. Gourdeau, B. Tseng, J. Drewe, S. X. Cai, *Bioorg. Med. Chem. Lett.* **2005**, *15*, 4745–4751.
- [38] W. Kemnitzer, J. Drewe, S. Jiang, H. Zhang, Y. Wang, J. Zhao, S. Jia, J. Herich, D. Labreque, R. Storer, K. Meerovitch, D. Bouffard, R. Rej, R. Denis, C. Blais, S. Lamothe, G. Attardo, H. Gourdeau, B. Tseng, S. Kasibhatla, S. X. Cai, *J. Med. Chem.* **2004**, *47*, 6299–6310.
- [39] H. Gourdeau, L. Leblond, B. Hamelin, C. Desputeau, K. Dong, I. Kianicka, D. Custeau, C. Bourdeau, L. Geerts, S. X. Cai, J. Drewe, D. Labrecque, S. Kasibhatla, B. Tseng, *Mol. Cancer Ther.* **2004**, *3*, 1375–1384.
- [40] S. Neamani, L. Moradi, M. Sun, *Appl. Surf. Sci.* **2019**, *504*, 144466–144477.
- [41] A. Thongni, P. T. Phanrang, A. Dutta, R. Nongkhlaw, *Synth. Commun.* **2022**, *52*, 43–62.
- [42] R. Sarma, M. M. Sarmah, K. C. Lekhok, D. Prajapati, *Synlett* **2010**, *19*, 2847–2852.
- [43] M. Mogharabi-Manzari, M. H. Ghahremani, T. Sedaghat, F. Shayan, M. A. Faramarzi, *Eur. J. Org. Chem.* **2019**, *2019*, 1741–1747.
- [44] A. Montagut-Romans, M. Boulven, M. Lemaire, F. Popowycz, *RSC Adv.* **2016**, *6*, 4540–4544.
- [45] K. Ramandeep, N. Fatima, S. Sahil, M. Samir, G. Manish Kumar, B. Preet Mohinder Singh, N. Kunal, *Med. Chem. Res.* **2015**, *24*, 3334–3349.
- [46] R. Ghahremanzadeh, T. Amanpour, A. Bazgir, *J. Heterocycl. Chem.* **2009**, *46*, 1266–1270.
- [47] B. Maheshwar Rao, G. Niranjana Reddy, T. Vijaikumar Reddy, B. L. A. Prabhavathi Devi, R. B. N. Prasad, J. S. Yadav, B. V. Subba Reddy, *Tetrahedron Lett.* **2013**, *54*, 2466–2471.
- [48] M. Baghernejad, S. Khodabakhshi, S. Tajik, *New J. Chem.* **2016**, *40*, 2704–2709.
- [49] H. R. Safaei, M. Shekouhy, S. Rahmanpur, A. Shirinfeshan, *Green Chem.* **2012**, *14*, 1696–04.
- [50] A. Hasaninejad, N. Golzar, M. Beyrati, A. Zare, M. M. Doroodmand, *J. Mol. Catal. A* **2013**, *372*, 137–50.
- [51] S. Riyaz, A. Indrasena, P. Dubey, *Indian J. Chem.* **2014**, *53B*, 1442–1447.

Manuscript received: February 22, 2022

Revised manuscript received: May 1, 2022